

LARGE AREA PHOTO-DETECTORS WITH MILLIMETER AND PICOSECOND RESOLUTION: SIMULATIONS

Valentin Ivanov[#], Thomas J. Roberts, Robert Abrams, Muons, Inc., Batavia, IL 60510, USA

Henry J. Frisch, University of Chicago, Chicago, IL 60637, U.S.A.

Abstract

Many measurements in particle and accelerator physics are limited by the time resolution with which individual particles can be detected. This includes particle identification via time-of-flight in major experiments like CDF at Fermilab and Atlas and CMS at the LHC, as well as the measurement of longitudinal variables in accelerator physics experiments. Large-scale systems, such as neutrino detectors, could be significantly improved by inexpensive, large-area photo detectors with resolutions of a few millimeters in space and a few picoseconds in time. Recent innovations make inexpensive, large-area detectors possible, with only minor compromises in spatial and time resolution. The G4beamline program [1] is one of the appropriate tools for simulation of low-energy physics processes. The set of specialized tools - MCPS [2], POISSON-2 [3] and Monte Carlo Simulator was used for numerical study of different photo multipliers.

INTRODUCTION

The entire package shown in Figure 1 is about 1 cm thick (along the particle axis, left-to-right in the figure), and the integrated-circuit readout electronics is mounted immediately behind it. By using square multichannel plates, this structure can be replicated to large areas with minimal dead zones at boundaries. Anode segmentation from a few millimeters to a centimeter or so is possible; the actual segmentation will depend on the matchup between the anode segments and the size and channel count of the readout electronics ICs.

Several aspects of this basic design were validated with using the code G4beamline. Currently available commercial multi-channel

plates (MCP) have almost adequate resolution, shown in Figure 2.

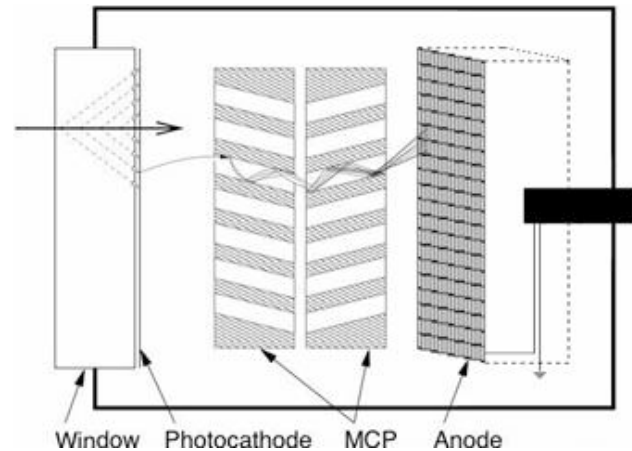


Figure 1. Cross-section of a fast timing detector. A relativistic charged particle produces Cherenkov radiation in the window. This radiation is converted into electrons by a photocathode at negative voltage. The electrons are accelerated into and produce a shower in the micro-channel plates (MCP), and the charge is deposited on the segmented anode and converted to an output signal.

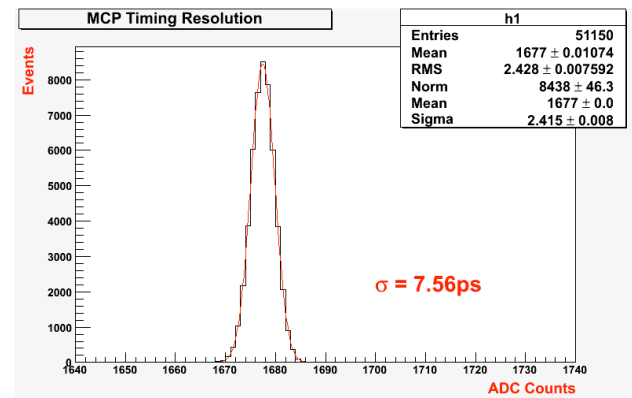


Figure 2. Measurement of the time difference between two commercial MCPs with 25µm pores. Data are for a 408nm laser with ~50 photoelectrons, at the laser test stand at Argonne (Hamamatsu PLP-10 picosecond laser system and a commercial CAMAC readout electronics system).

[#]ivanov@muonsinc.com

CHEVRON-TYPE MCP SIMULATION

Here we present briefly the methodic by Y. Kulikov [5]. The elementary current coming to the channel surface is

$$dI'_{02} = I_{02} \omega'_{z0}(z'_{02}) K'_{02}(\varepsilon'_{02}, \Omega'_{02}, \gamma'_{02}) d\varepsilon'_{02} d\Omega'_{02} d\gamma'_{02} r'_{02} dr'_{02}.$$

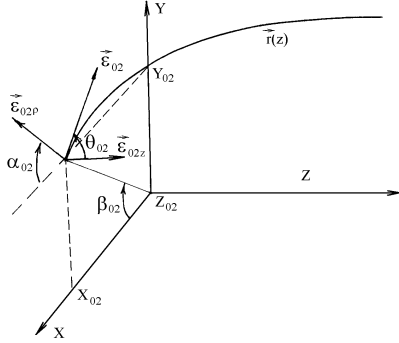


Figure 3. Coordinate system in the micro channel area.

This current creates a cascade of secondary particles emitted by the channel wall, which is characterized by the current distribution

$$\omega_{z1}(z_{12} - z_{02}) = \frac{W_{z1}(z_{12} - z_{02})}{k_1}$$

and by the amplification ratio

$$k_1 = \int_{L_1}^{L_1+L_2} W_{z1}(z_{12} - z_{02}) dz_{12}.$$

The elementary current before the 2nd cascade is

$$dI'_{12} = I'_{12} \omega'_{z1}(z'_{12} - z_{02}) K'_{12}(\varepsilon'_{12}, \Omega'_{12}, \gamma'_{12}) d\varepsilon'_{12} d\Omega'_{12} d\gamma'_{12} dz'_{12}.$$

The current-distribution function on the surface before the 2nd cascade is described by a formula

$$\omega'_{z1}(z'_{12} - z_{02}) = \int_{L_1}^{L_1+L_2} \omega_{z1}(z'_{12} - z_{02}) \omega'_z(z'_{12} - z_{12}) dz_{12},$$

and the current-distribution function on the surface after the 2nd cascade is

$$dI_{22} = I_{22} \omega_{z2}(z_{22} - z_{02}).$$

As the result we obtain the recursive correlations $I_{n2} = I_{02} k_1 k_2 \dots k_n$,

$$\omega'_{zn}(z'_{n2} - z_{02}) = \int \dots \int \omega_{z1}(z_{12} - z_{02}) \omega'_z(z'_{12} - z_{12}) \dots \omega'_z(z'_{n2} - z_{n2}) dz_{12}.$$

$$W_{zn}(z_{n2} - z_{02}) = \int \dots \int \omega_{z1}(z_{12} - z_{02}) \omega_z(z_{22} - z_{12}) \dots \omega_z(z_{n2} - z_{n-1,2}) dz_{12}.$$

$$\omega_{zn} = \frac{W_{zn}}{k_n}, \quad k_n = \int W_{zn}(z_{n2} - z_{02}) dz_{n2}.$$

Total elementary current is described by a

sum

$$dI_{\Sigma} = dI_{02} + dI_{12} + \dots + dI_{n2},$$

where

$$dI_{n2} = I_{n2} \omega_{zn}(z_{n2} - z_{02}) K_{n2}(\varepsilon_{n2}, \Omega_{n2}, \gamma_{n2}) d\varepsilon_{n2} d\Omega_{n2} d\gamma_{n2}$$

Total current from the channel surface is

$$I_{\Sigma} = I_{02} k_{\Sigma},$$

and total gain factor of MCP is given by a formula $k_{\Sigma} = k_1 + k_1 k_2 + \dots + k_1 k_2 \dots k_n$.

The particle trajectory in the uniform field E_2 is given by formula

$$z'_{02} = z_{02} + \frac{E_2}{4\varepsilon_{02} \sin^2 \theta_{02}} \left[\sqrt{R_0^2 - r_{02}^2 \sin^2(\alpha_{02} - \beta_{02})} - r_{02} \cos(\alpha_{02} - \beta_{02}) \right]^2 + \left[\sqrt{R_0^2 - r_{02}^2 \sin^2(\alpha_{02} - \beta_{02})} - r_{02} \cos(\alpha_{02} - \beta_{02}) \right] \text{ctg} \theta_{02}.$$

We use the Guest's formula for true secondary electron emission [6]

$$\sigma(\theta, \varepsilon) = \sigma_{\max} \left(\frac{\varepsilon - \sqrt{\cos \theta}}{\varepsilon_{\max}} \right)^{\beta} \exp \left[\alpha(1 - \cos \theta) + \beta \left(\frac{\varepsilon - \sqrt{\cos \theta}}{\varepsilon_{\max}} \right) \right],$$

where σ_{\max} - maximal value for the secondary emission ration in normal fall the electrons on the surface, ε_{\max} - correspondent value for the collision energy, θ - angle between the velocity vector of primary electron and normal vector on the surface, α - absorbing ratio of the wall, β - parameter of the emission model. From the experimental data the absorbing ratio $\alpha = 0.62$, and

$$\beta = \begin{cases} 0.55 \leq \beta \leq 0.65, & \varepsilon < \varepsilon_{\max}, \\ 0.25, & \varepsilon > \varepsilon_{\max}. \end{cases}$$

This methodic was used to simulate the MCP "Planacon" by Burle/Photonics [7] shown in Figure 4. The results of numerical simulations presented in Figures 5-7.

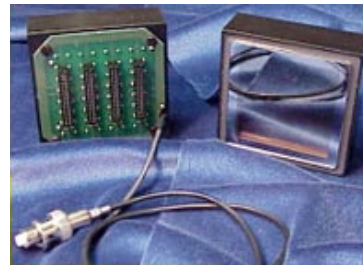


Figure 4. Chevron-type photo multiplier 85022. The MCP area is 2''x2'', with 1024 anodes, all equally spaced by 1.6 mm.

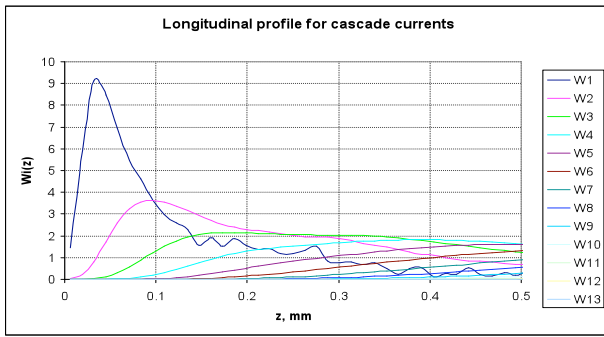


Figure 5. Current distribution for the cascades.

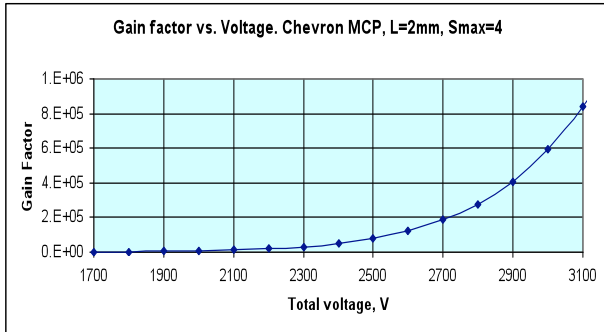


Figure 6. Gain factor vs. MCP voltage.

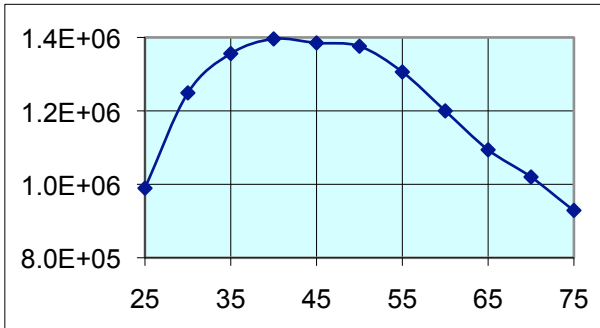


Figure 7. Gain factor vs. ratio L/D. L is length of pore, D is its diameter.

FUNNEL-TYPE MCP SIMULATION

We have several ideas for improving the open-area ratio and better determining the place of first strike, including making the entrance to the channel into a funnel, as shown in Figure 8, so that the electron strikes the surface of the funnel and secondary electrons are sucked into the channel. Alternatively, the funnel could be directly coated with the photo-cathode material, with the photo-electron or electrons then initiating the shower in the channel, as shown in the simulation in Figure 9. The funnel solution is attractive in that it hides the photo-cathode

from ion feedback, i.e. ions that are created on the channel walls and accelerated back up the channel. These ions are a cause of aging of MCP's, and can be a problem at high gain. Figures 9-10 demonstrate the dependence of photo-electron capturing vs. the funnel diameter and photo cathode resistance.

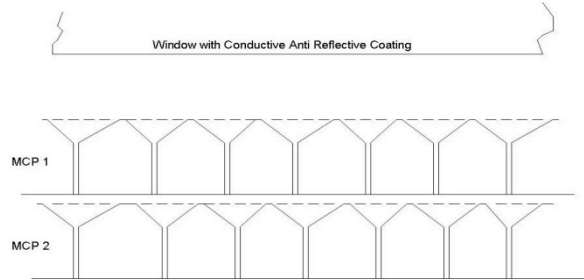


Figure 8. A sketch of the funnel solution.

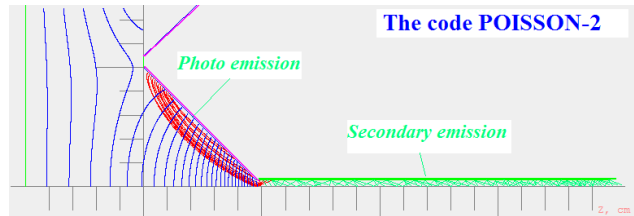


Figure 9. Primary photo-electrons (red), secondaries (green) and equi-potentials (blue) in funnel MCP.

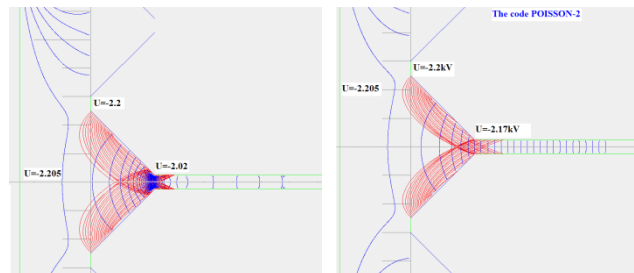


Figure 10. Capturing of photo electrons can be optimized by varying the resistance of photo cathode.

REFERENCES

- [1] G4beamline: <http://g4beamline.muonsinc.com>.
- [2] V. Ivanov, Micro Channel Plate Simulator, User's Guide, Muons, Inc., 2009.
- [3] V. Ivanov. Proc. 2nd Int. Conf. on Computations in Electromagnetism, Nottingham, May 13-15, 1994.
- [4] V. Ivanov, Z.Insepov, "Micro Channel Plate Simulations: State of the Art", Pico-Second Workshop VII, February 26-28, 2009; Argonne National Lab.
- [5] Y. Kulikov, Radiotekhnika i Svetotekhnika, **4**, 1967, pp.376-380.
- [6] A.J. Guest, ACTA Electronica, V.14, N1, 1971, p. 85.
- [7] http://www.burle.com/prod_showcase.htm